

Detection of Transmission Line Faults by Wavelet Based Transient Extraction

P. Venugopal Rao¹, Shaik Abdul Gafoor², and C. Venkatesh¹

¹Electrical and Electronics Engineering Department, SR Engineering College, Warangal, India

Email: pendyalavenu@yahoo.com

²Electrical and Electronics Engineering Department, Bapatla Engineering College, Bapatla, India

Email: saadgafoor@yahoo.com, challacvs@yahoo.com

Abstract— In this paper, a novel technique is applied to detect fault in the transmission line using wavelet transform. Three phase currents are monitored at both ends of the transmission line using global positioning system synchronizing clock. Wavelet transform, which is very fast and sensitive to noise, is used to extract transients in the line currents for fault detection. Fault index is calculated based on the sum of local and remote end detail coefficients and compared with threshold value to detect the fault. Proposed technique is tested for various faults and fault inception angles. Simulation results are presented showing the selection of proper threshold value for fault detection.

Index Terms— Wavelet transform, transmission line faults, power system protection, fault transients, multiresolution analysis

I. INTRODUCTION

Transmission lines exposed to various faults are designed with distance protection scheme. The main principle of this technique is to calculate the impedance between the relay and fault points; the apparent impedance is then compared with the relay trip characteristic to ascertain whether it is an internal or external fault. Microprocessor based distance relays have been broadly applied to transmission lines protection. The calculation of line impedance has been carried out in difference equations [1], [2] or using phasor obtained by Fourier algorithms [3], [4]. To set a distance relay, it is necessary to determine the reach of its setting. A distance relay does not aim to locate a fault but instead its objective is to determine whether a fault is within or outside the intended protection zone. Methods exploiting travelling wave components to achieve ultra high speed protection have also been proposed [5], [6], while their performance needs further evaluation and, where necessary, improvement [7]. Wavelet analysis as a powerful tool for signal processing can be applied to effectively overcome difficulties of the travelling wave protection techniques [8]–[11]. By virtue of the variable length data window of the wavelet transform (WT), it is possible to detect and characterize closed singularities of nonstationary signals. The wavelet transform can also be employed for preprocessing of input data to improve the performance of artificial-neural-network (ANN)-based algorithms [11]. In [12] principal component analysis technique is proposed to identify the dominant pattern of the signal preprocessed by the wavelet transform. This way,

the extracted information of the voltage and current signals by wavelet transform at different scales is utilized. This technique improves the capability of traveling-wave detection especially for the faint and close-in faults. The proposed position protection algorithm is based on polarity, magnitude, and time interval between the arriving waves, and can rapidly identify most of the faults occurring inside the protected zone. In this paper, wavelet based multiresolution analysis is used for detection of fault based on detail-1 coefficients of current signals at both the ends of line. Transients are introduced due to fault in the currents of faulted phase. These high frequency components are easily extracted by wavelet analysis. A fault index is then calculated by combining the detail-1 coefficients of three phase currents monitored at both ends of the transmission line using global positioning system synchronizing clock. The details of the proposed scheme are described and simulation results are presented for detection of various faults at different fault distance and inception angles. Results show that a common threshold fault index is used to detect the fault in the line.

II. WAVELET TRANSFORMS

Wavelet transform is useful in detecting and extracting disturbance features of various types of electric power quality disturbances because it is sensitive to signal irregularities. Wavelet analysis expands functions not in terms of trigonometric polynomials but in terms of wavelets, which are generated in the form of translations and dilations of a fixed function called the mother wavelet. A mother wavelet is a function that oscillates, has finite energy and zero mean value. Compared with Fourier transform, wavelet can obtain both time and frequency information of signal, while only frequency information can be obtained by Fourier transform. The signal can be represented in terms of both the scaling and wavelet function [8] as follows:

$$f(t) = \sum_n c_j(n)\varphi(t-n) + \sum_{j=0}^{J-1} \sum_n d_j(n)2^{j/2}\psi(2^j t-n) \quad (1)$$

Where c_j is the J level scaling coefficient

d_j is the j level wavelet coefficient

$\varphi(t)$ is scaling function

$\psi(t)$ is wavelet function

J is the highest level of wavelet transform

t is time

Each wavelet is created by scaling and translation operations of mother wavelet. Wavelet theory is expressed by

Corresponding author: P. Venugopal Rao

continuous wavelet transformation as

$$CWT_{\psi} x(a, b) = W_x(a, b) = \int_{-\infty}^{\infty} x(t)\psi^*_{a,b}(t)dt \quad (2)$$

where $\psi_{a,b}(t) = |a|^{1/2} \psi(\frac{t-b}{a})$,

a (scale) and b (translation) are real numbers.

For discrete-time systems, the discretization process leads to the time discrete wavelet series as

$$DWT_{\psi} x(m, n) = \int_{-\infty}^{\infty} x(t)\psi^*_{m,n}(t)dt \quad (3)$$

where $\psi^*_{m,n}(t) = a_o^{-m/2} \psi(\frac{t-nb_o a_o^m}{a})$,

$a = a_o^m$ and $b = nb_o a_o^m$

In Multi resolution analysis (MRA), wavelet functions and scaling functions are used as building blocks to decompose and construct the signal at different resolution levels. The goal of MRA is to develop representations of a signal at various levels of resolution. MRA is composed of 2 filters in each level which are low pass filter and high pass filter. MRA can be shown as in Fig. 1. Wavelet coefficients obtained from high pass filter are called detail coefficients and coefficients at low pass filter are called approximation coefficients. Transients generated during faults are of high frequency components which can easily be extracted from level 1 wavelet coefficients.

III. FAULT PROTECTION ALGORITHM

In this paper, wavelet analysis is used to detect the fault in the transmission line. Fig. 2 shows system configuration used for analysis. A 100 kms transmission line of rating 138kV, 100MW, 60Hz is fed from both ends. Synchronized sampling of three phase currents and voltages is carried out at both the ends with the help of a GPS satellite. Wavelet analysis of these sampled signals is performed and level-1 detail coefficients are used to calculate fault index and detect fault.

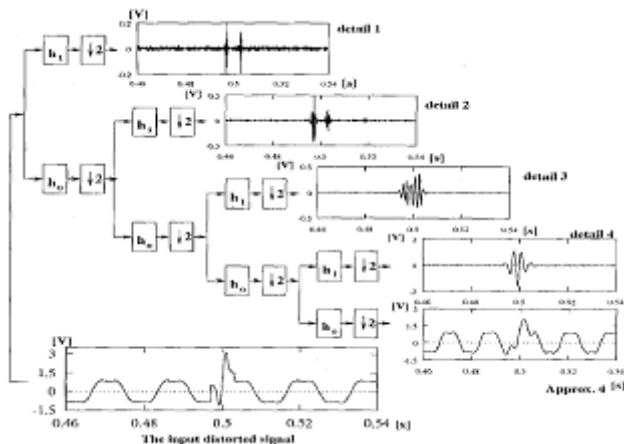


Figure 1. Four level multi resolution signal decomposition of a signal.

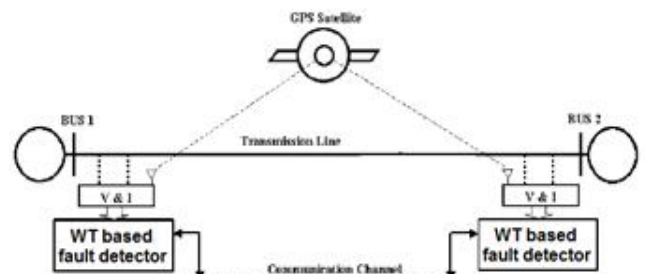
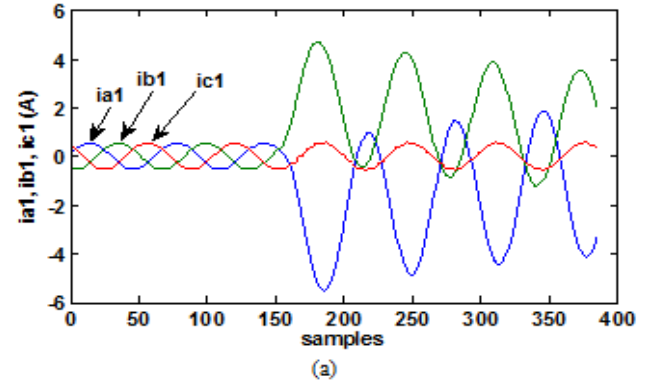
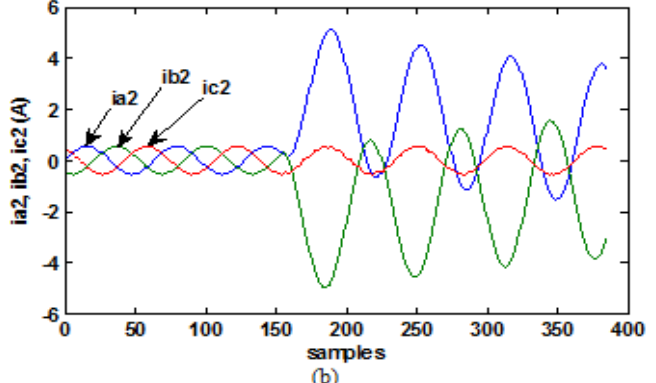


Figure 2. Transmission line system with FACTS device implemented with proposed scheme



(a)



(b)

Figure 3. Current waveforms during ABG fault at 20% line length from bus 1 (a). Three-phase currents at Bus-1 and (b). Three-phase currents at Bus-2

Two-phase to ground fault is considered here for fault index calculation. Figs. 3(a) and (b) show the three-phase currents at bus-1 and bus-2, respectively for ABG fault. Currents in phase A and B increase during fault. These sampled currents are then analyzed with Debauches' wavelet to obtain level-1 detailed coefficients (CD1) over a moving window of half-cycle length. Level-1 detail coefficients for phase-A, B and C currents (CD1_ia1, CD1_ib1, CD1_ic1) at bus-1 are shown in Figs. 4(a), (b) and (c) respectively. Level-1 detail coefficients for phase-A, B and C currents (CD1_ia2, CD1_ib2, CD1_ic2) at bus-2 are shown in Figs. 4(d), (e) and (f) respectively. These coefficients indicate high frequency components in the currents due to fault. Currents in faulted phase indicate a large magnitude of coefficients which are used to detect fault.

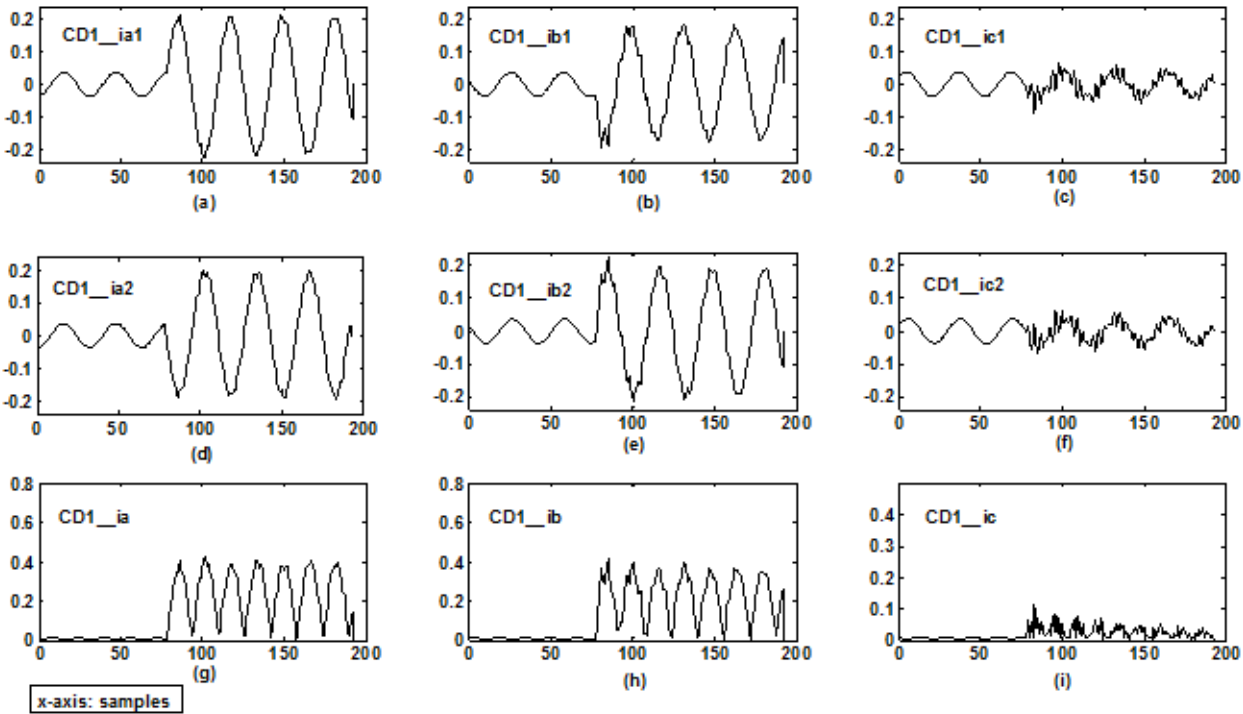


Figure 4. Wavelet analysis of three-phase currents, (a), (b), (c). Level-1 detailed coefficients of bus-1 phase-A, phase-B current and phase-C currents respectively, (d), (e), (f). Level-1 detailed coefficients of bus-2 phase-A, phase-B and phase-C currents respectively, (g), (h), (i).

Effective detail coefficients of phase-A, phase-B current and phase-C currents respectively

The detail coefficients received from the remote bus (bus-2) are added to the local bus (bus-1) detail coefficients. Variation of these effective detail coefficients ($CD1_{ia}$, $CD1_{ib}$, $CD1_{ic}$) are shown in Figs. 4(g)-(i).

Fault index is then calculated in each phase as

$$I_{fl} = \sum |DI_E| \quad (4)$$

Variation of fault index in each of the three-phases for ABG fault is shown in Fig. 5. It is clear from the figure that fault index is large in faulted phases as compared to that in healthy phase. A threshold value (I_{TH}) is then set such that $I_{TH} < I_{fl}$ of faulted phase and $I_{TH} > I_{fl}$ of healthy phase. This algorithm is tested for various faults and a common threshold value is selected.

IV. SIMULATION RESULTS

The proposed algorithm is tested for all types of faults, considering variations in fault locations and fault inception angles in the range of 0-180° for the simulation circuit of the system shown in Fig. 6. Simulation is performed for an LLG fault at every 20kms of the line and at various fault inception angles. Fig. 7 shows variation of fault index, I_{fl} for ABG fault applied at every 20kms distance on the line and fault inception angles of 0°, 30°, 60°, 90°, 150° and 180°. It is clearly observed from the figure that fault index is large in faulted phases A and B compared to fault index in healthy phase C. This shows that extracting transients from the fault currents using wavelets helps to detect fault and faulted phase. To compare the fault index for various types of faults, simulation is performed for all the faults. Fig. 8 shows the variation of fault index for AG, BG, ABG, AB, ABCG and ABC faults at different

distances and for fault inception angle at 30°. It can be seen that transients in faulted phases are high compared to healthy phase. From Figs. 7 and 8 it is possible to set a threshold value between the fault index for fault and healthy phases.

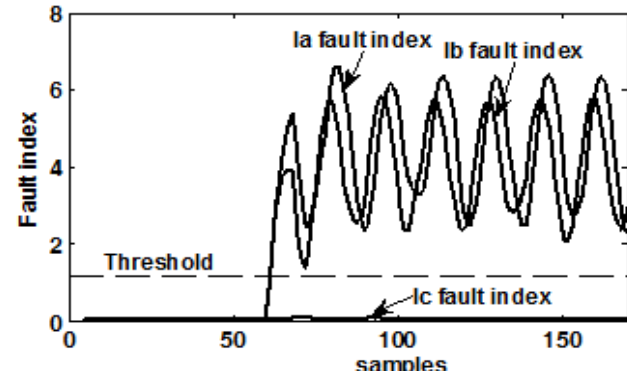


Figure 5. Variation of Fault Index in due to ABG fault

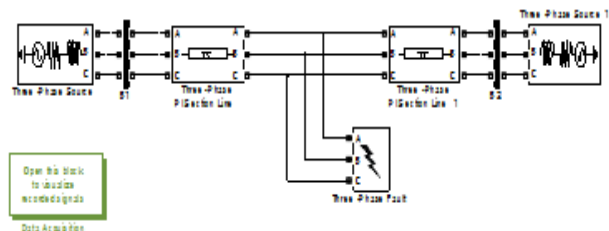
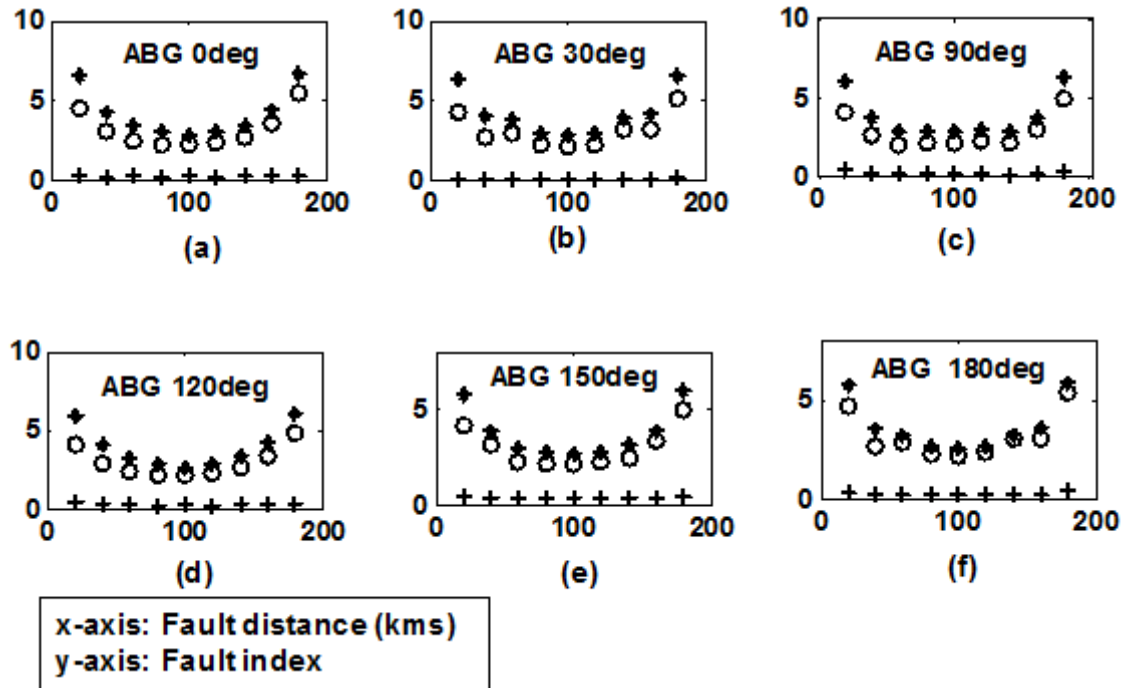
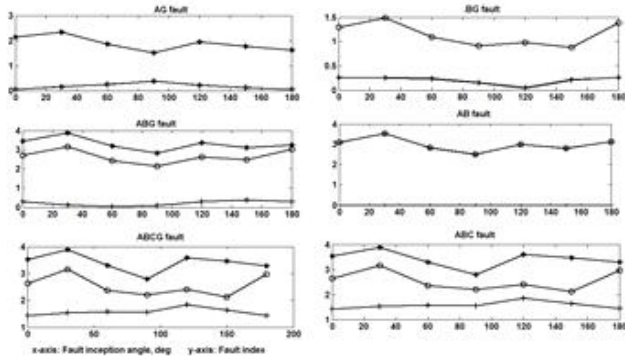


Figure 6. Simulation circuit of the transmission system used for testing the proposed algorithm



* Phase A fault index, 0 Phase B fault index, + Phase C fault index

Figure 7. Variation of fault index for ABG fault



* Phase A fault index, 0 Phase B fault index, + Phase C fault index

Figure 8. Variation of fault index connected and fault at 140kms distance from bus1 for various faults

Fault index is calculated for case studies of all possible faults at various points on the line and at various inception angles. These values are tabulated in Table I. The values listed are minimum fault index possible for faulty phase and maximum fault index possible for healthy phase. For example considering ABG fault from Table I, minimum fault index in phases A and B are 2.5397 and 2.0021 respectively and maximum fault index in phase C is 0.4557. Fault index calculated from transients show that index values are larger for faulty phase currents compared to index of healthy phase current. The proposed algorithm is therefore having an edge over fundamental impedance calculation method which is normally employed with distance relay. From Table I minimum fault index in phase A (I_{fla_min}) is 1.3589 which is obtained considering for all possible faults with phase A involved i.e., AG fault, ABG fault, CAG fault, AB fault, CA fault, ABCG fault and ABC fault. Maximum fault index in phase A (I_{fla_max}) is 0.5794 which is obtained for faults with healthy phase A

i.e., BG fault, CG fault, BCG fault and BC fault. Similarly minimum and maximum fault index for Phase B and C (I_{flb_min} , I_{flc_min} , I_{flb_max} , I_{flc_max}) are identified. Proper threshold index (I_{TH}) is then set between minimum fault index (I_{fl_min}) and maximum fault index (I_{fl_max}) of all faults as

$$I_{TH} < I_{fl_min} \text{ and } I_{TH} > I_{fl_max} \quad (5)$$

where $I_{fl_min} = \min(I_{fla_min}, I_{flb_min}, I_{flc_min})$ and

$I_{fl_max} = \max(I_{fla_max}, I_{flb_max}, I_{flc_max})$

From this case study, $I_{fl_min} = 0.7393$ and $I_{fl_max} = 0.5794$ (from Table 1). A common threshold index $I_{TH} = 0.65$ may be set between I_{fl_min} and I_{fl_max} . Fault in a phase is detected when the fault index exceeds 0.65. The feature of this algorithm is that transients are easily extractable using wavelet analysis and provides a common setting of threshold index.

TABLE I. FAULT INDICES FOR VARIOUS FAULTS

Fault	Phase-A Index		Phase-B Index		Phase-C Index	
	Min.	Max.	Min.	Max.	Min.	Max.
AG	1.3589*	-	-	0.5715+	-	0.5559-
BG	-	0.4988	0.7690*	-	-	0.4837
CG	-	0.5794+	-	0.5577	0.7393*	-
ABG	2.5397	-	2.0021	-	-	0.4557
BCG	-	0.5179	1.1915	-	0.8084	-
CAG	1.9323	-	-	0.4447	1.6221	-
AB	2.3390	-	2.3532	-	-	0.0253
BC	-	0.0548	0.8212	-	0.8315	-
CA	1.8047	-	-	0.0405	1.8366	-
ABCG	2.7743	-	1.7837	-	1.2769	-
ABC	2.7743	-	1.7837	-	1.2769	-

* indicates the lowest fault index when the phase is faulted

+ indicates the largest fault index when the phase is healthy

V. CONCLUSIONS

An algorithm for detection of faults in the transmission line is proposed based on transient component extraction of currents. Fault index calculated from detail-1 coefficients of currents are clearly separable for fault and healthy phases. This provides an easy selection of threshold to detect fault in the line. Simulation results presented for various faults at different distances and inception angles show that a common threshold is set to detect a fault in the transmission line.

REFERENCES

- [1] G. B. Gilcrest, G. D. Rockefeller, and E. A. Udren, "High speed distance relaying using a digital computer, part 1—System description," *IEEE Trans. Power App. Syst.*, vol. PAS-91, no. 3, pp. 1235–1243, 1972.
- [2] B. J. Mann and I. F. Morrison, "Digital calculation of impedance for transmission line protection," *IEEE Trans. Power App. Syst.*, vol. PAS-90, no. 1, pp. 270–278, 1971.
- [3] D. L. Waikar, S. Elangovan, and A. C. Liew, "Fault Impedance Estimation Algorithm for Digital Distance Relaying," *IEEE Trans. Power Delivery*, vol. 9, no. 3, pp. 1375–1383, Jul. 1994.
- [4] Z. Y. Xu, "An ultra-high speed distance protection algorithm," in *Proc. IEEE and CSEE Int. Conf. Power System Technology*, Beijing, China, Oct. 1994, pp. 1149–1152.
- [5] P. A. Crossley and P. G. McLaren, "Distance protection based on travelling waves," *IEEE Trans. Power App. Syst.*, vol. 102, no. 9, pp. 2971–2983, Sep. 1983.
- [6] E. H. Shehab-Eldin and P. G. McLaren, "Travelling wave distance protection- problem areas and solutions,"
- [7] V. Pathirana and P. G. McLaren, "A hybrid algorithm for high speed transmission line protection," *IEEE Trans. Power Del.*, vol. 20, no. 4, pp. 2422–2427, Aug. 2005.
- [8] W. Chen, O. P. Malik, X. Yin, D. Chen, and Z. Zhang, "Study of wavelet-based ultra high speed directional transmission line protection," *IEEE Trans. Power Del.*, vol. 18, no. 4, pp. 1134–1139, Oct. 2003.
- [9] D. J. Zhang, Q. H. Wu, Z. Q. Bo, and B. Caunce, "Transient positional protection of transmission lines using complex wavelets analysis," *IEEE Trans. Power Del.*, vol. 18, no. 3, pp. 705–710, Jul. 2003.
- [10] M. Gilany, D. K. Ibrahim, and T. Eldin, "Travelling-wave based fault location scheme for multiend-aged underground cable system," *IEEE Trans. Power Del.*, vol. 22, no. 1, pp. 82–89, Jan. 2007.
- [11] F. Martin and J. A. Aguado, "Wavelet-based ANN approach for transmission line protection," *IEEE Trans. Power Del.*, vol. 18, no. 4, pp. 1572–1574, Oct. 2003.
- [12] Peyman Jafarian, Majid Sanaye-Pasand, "A Travelling-Wave-Based Protection Technique Using Wavelet/PCA Analysis" *IEEE Trans. Power Del.*, vol. 25, no. 2, pp. 588 - 599, Apr. 2010.